

Quantum universality of phase transitions

Shpend Mushkolaj

Abstract

The most astonishing properties of condensed matter are the formation of collective quantum states of superconductivity, magnetic order, electric order and crystalline order. In this paper, new universal formulas for transition temperatures are derived, that depend simply on atom-atom distances, atomic masses and electron masses. The universality of these formulas is tested by comparing the calculated values and experimental data for critical temperatures of different systems and phases.

Keywords: Transition temperatures; Superconductivity; Magnetism; Spontaneous electric polarization; Melting

1. Introduction

In condensed matter physics, superconductivity (high- T_c) is considered as one of the most profound problems. The exaggeration has gone so far that it is compared with the problems of dark energy, extra dimensions and secret of life ¹. A complete theory of superconductivity is still missing, since the theory of Bardeen, Cooper and Schrieffer (BCS) is applicable only to the so-called conventional superconductors. It is believed that a minor revolution is needed to understand high-temperature superconductivity ². Until now, there is no universal model that is able to describe conventional and high- T_c superconductivity.

On the other hand, there is an overconfidence in the theoretical knowledge of the collective quantum state of magnetic order, although there are still many open problems that can not be solved with our actual theoretical models. For example, ferromagnetism of iron, which is the basic example of magnetic order, is still a puzzling problem where some experimental data are well interpretable in terms of itinerant-electron (band theory) model and other data, in terms of localized-electron model ³. Until now, no theoretical model has been able to calculate the experimental Curie temperature of Fe (1043 K) exactly, or calculate and explain the origin of the phase transition at 17.5 K in URu₂Si₂. The weak high-temperature ferromagnetism of

CaB₆ and LaB₆ is also still inexplicable⁴⁻⁶. Today, a universal model that can describe the magnetic order in insulators, semiconductors and metals is missing.

The spontaneous electric polarization (electric order) is one of the fundamental problems of solid-state physics that is theoretically less understood. With the actual theoretical models, we are not able to predict critical temperatures for ferroelectric or anti-ferroelectric systems. For instance, the formula for calculating the transition temperatures T_c , which is derived from the mean field theory, is given as:

$$T_c = C_{C-W} \frac{J_0 V_{uc}}{4\pi p_z^2}$$

where C_{C-W} , J_0 , V_{uc} , and p_z represent the Curie-Weiss constant, the interaction of a particle with all other particles being located within a large interaction radius (r_0) (*i.e.* $r_0 \gg$ lattice parameters), volume of the unit cell and the dipole moment respectively. For displacive-type cubic crystals with the electric dipoles located in the centers of the unit cells, the Lorentz factor becomes $J_0 V_{uc} / p_z^2 = 4\pi/3$, and the above formula for T_c is transformed into:

$$T_c = \frac{C_{C-W}}{3}.$$

Table I provides a list of critical temperatures for different ferroelectric materials.

TABLE I. Different compounds, type of electric order, experimental Curie temperatures and Curie-Weiss constants. These data were obtained from Ref. ⁷.

Compound	Type of order	T_c^{exp} (K)	C_{C-W} (K)
TGS	Order-disorder	322	3200
NaNO ₂	Order-disorder	473	5000
KH ₂ PO ₄	Order-disorder	123	3600
BaTiO ₃	Displacive	400	170000

We see that the above equation is fulfilled only in order of magnitude for order-disorder type, while for the displacive type ferroelectric of BaTiO₃ there is no agreement with the experimental results. Until now, there is no universal model that is able to describe the electric order of displacive type and order-disorder type.

Today, we do not have the right theoretical tool that is able to predict the crystallization (melting) temperatures of solid materials.

Twenty-four hundred years ago, Leucippus and Democritus developed a mechanistic view of nature in which every material phenomenon was seen as a product of atom collisions. Pluto hated this opinion so much that he proposed five years of solitary confinement for people who

held these heretical thoughts, followed by death if they had not reformed. These heretical thoughts (or perhaps it would be better to say modern ideas) together with the fundamental conservation laws of energy and momentum, Heisenberg's uncertainty principle and Schrödinger's equation, are the basic concepts that will be used in the universal model presented here, namely, the model of elastic atom-atom and electron-atom collisions. It will be proven that the model is universal and it can qualitatively and quantitatively explain all types of phase transitions.

This paper is organized as follows: in Sec. II, the universal formulas for critical temperatures are derived. In Sec. III, the universality of these formulas are confirmed by comparing experimental values with experimental data for different phase transitions. In Sec. IV, a discussion of the universal model is presented.

2. Derivation of the T_C formulas

Let us start from the fact that matter is electrically neutral and the total number of positive protons and negative electrons are equal. All the attractive and repulsive Coulomb forces cancel each other from the microscopic scales, *i.e.* neutron, atom, unit crystalline cells, etc., to the macroscopic scales. Based on this fact, only masses of electrons and atoms are considered, but not their electrical charges. First, I assume that at critical temperatures the electron-atom and atom-atom collisions are elastic, *i.e.*, the kinetic energy and momentum are conserved before, during and after collisions. My second assumption is that during elastic collisions the masses of microscopic particles (electron-atom and atom-atom) are mixed into $\sqrt{M_1 M_2}$ and these mass mixtures are electrically neutral.

2.1. Elastic atom-atom and electron-atom collisions

Generally, in the theory of elastic lattice waves the atomic radii are neglected and the minimum possible wavelength (λ'_{min}) is given by twice the equilibrium separation a between atoms, $\lambda'_{min} = 2a$. If we consider the fact that atomic and ionic radii in crystalline structures are $R_a > 0$, the minimal vibration amplitudes get smaller than $2a$, $\lambda_{min} = 2(a - R_a) < \lambda'_{min}$. In the following, the atomic displacements with wavelength $2(a - R_a)$ are called elastic atom-atom collisions. In the case of elastic electron-atom collisions, the centers of electron and atom masses are allowed to overlap, and therefore, we do not need to know the atomic radii.

The kinetic energies and momentums for particles (*i.e.* atoms or electrons) with masses M_1 and M_2 before and after elastic collisions are given by:

$$\left(\frac{p_{M_1}^2}{2M_1}, M_1 V_{M_1} \right) \text{ and } \left(\frac{p_{M_2}^2}{2M_2}, M_2 V_{M_2} \right), \quad (1)$$

where $M_1, M_2, p_{M_1}, p_{M_2}, V_{M_1}$ and V_{M_2} represent the corresponding particle masses, momentums and speeds. To permanently transmit the entire kinetic energy and momentum from particle with mass M_1 to particle with mass M_2 and vice versa, the energy-momentum laws also need to be fulfilled during collision time. Since both atoms vibrate simultaneously, we can not distinguish them in the interval $2(a - (R_1 + R_2))$. The mass of this electrically neutral *particle₁-particle₂* mixture is $\sqrt{M_1 M_2}$ (see Fig. 1a) in a-direction. The kinetic energy and momentum for this neutral mixture are given by:

$$\frac{\vec{p}_{M_1} \cdot \vec{p}_{M_2}}{2\sqrt{M_1 M_2}} = \sqrt{M_1 M_2} \frac{\vec{V}_{M_1} \cdot \vec{V}_{M_2}}{2} \quad (2)$$

$$\sqrt{M_1 M_2} \sqrt{(\vec{V}_{M_1} + \vec{V}_{M_2})^2} = \sqrt{M_1 M_2} \sqrt{V_{M_1}^2 + V_{M_2}^2 + 2\vec{V}_{M_1} \cdot \vec{V}_{M_2}} \quad (3)$$

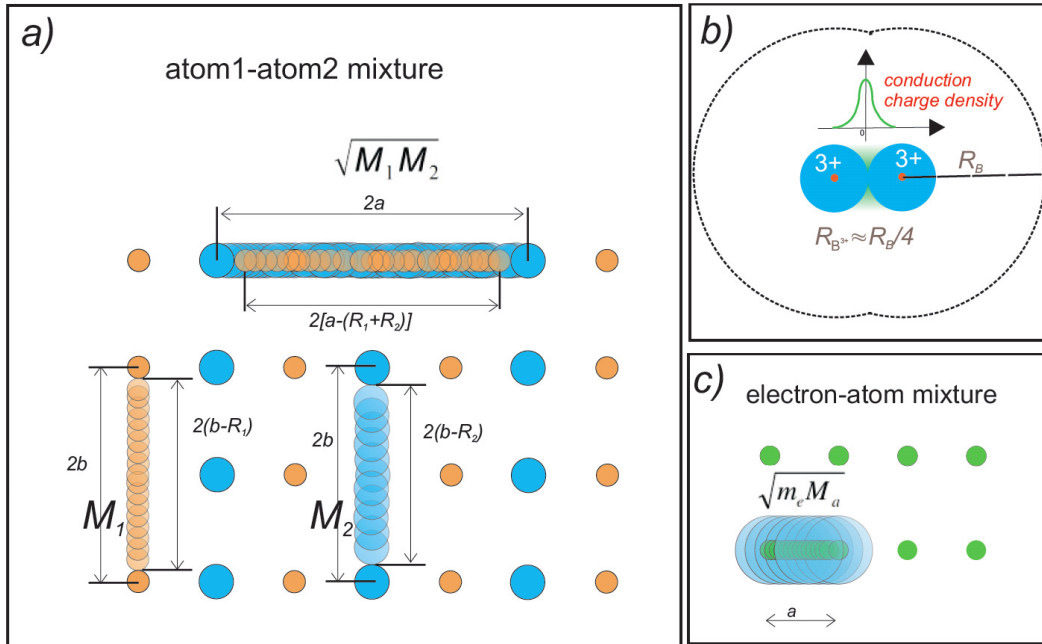


Fig. 1: a) A rectangular 2D lattice with lattice parameters a and b and atoms with masses M_1 (red) and M_2 (blue). In a -direction are shown elastic $atom_1$ - $atom_2$ collisions, in b -direction elastic $atom_1$ - $atom_1$ and $atom_2$ - $atom_2$ collisions. b) During elastic B^{3+} cation-cation collision, conduction charges are attracted and the maximal density is at the contact point of cations. Since repulsive and attractive Coulomb forces cancel each other, they do not slow down or

accelerate cations. This conduction charge density propagates simultaneously with elastic cation-cation collisions. c) A mixture of electron-atom masses during elastic collisions. The centers of the electron (blue) and atom (green) masses overlap during collision.

During elastic collisions, the kinetic energy and the total momentum are conserved before, during and after collisions, and are given as follows:

$$\frac{p_{M_1}^2}{2M_1} = \frac{p_{M_2}^2}{2M_2} = \frac{\vec{p}_{M_1} \cdot \vec{p}_{M_2}}{2\sqrt{M_1 M_2}} \quad (4)$$

$$(|\vec{p}_{M_1}| + |\vec{p}_{M_2}|)_{before} = (\sqrt{M_1 M_2} \sqrt{V_{M_1}^2 + V_{M_2}^2 + 2V_{M_1} \cdot V_{M_2}})_{mix} = (|\vec{p}_{M_1}| + |\vec{p}_{M_2}|)_{after} \quad (5)$$

During collisions, the kinetic energy and total momentum conservation laws are fulfilled for $\alpha = 0^\circ$, i.e.

$$\vec{p}_{M_1} \cdot \vec{p}_{M_2} = |\vec{p}_{M_1}| |\vec{p}_{M_2}| \cos \alpha = |\vec{p}_{M_1}| |\vec{p}_{M_2}|, \quad \vec{V}_{M_1} \cdot \vec{V}_{M_2} = |\vec{V}_{M_1}| |\vec{V}_{M_2}| \cos \alpha = |\vec{V}_{M_1}| |\vec{V}_{M_2}|. \quad (6)$$

This means that the momentum and speed vectors of *particle*₁ and *particle*₂ during collisions are aligned in the same direction.

Since superconductivity and magnetic order are pure quantum-mechanic phenomena, the propagation of *particle*₁-*particle*₂ mixture will be described quantum-mechanically. The Hamiltonian of the electrically neutral particle mixture is comprised solely of the kinetic term and expressed as:

$$\hat{H} = \frac{-\hbar^2}{2\sqrt{M_1 M_2}} \frac{\partial^2}{\partial x^2} \quad (7)$$

The mixture propagation is given by the time-dependent Schrödinger wave equation:

$$\frac{-\hbar^2}{2\sqrt{M_1 M_2}} \frac{\partial^2}{\partial x^2} \Psi(x, t) = i\hbar \frac{\partial}{\partial t} \Psi(x, t) \quad (8)$$

Below the transition temperature, the quantum states of the mass mixtures are described by the plane wave functions of the form:

$$\Psi(x, t) = e^{i(\pm kx - \frac{\Delta E t}{\hbar})} \quad \text{and} \quad \Psi'(x, t) = e^{i(\pm k'x - \frac{\Delta E' t}{\hbar})} \quad (9)$$

After inserting the plane wave functions into the above Schrödinger equation, we get:

$$\Delta E = \frac{\hbar^2}{4\pi\sqrt{M_1 M_2}} k^2 \quad \Delta E' = \frac{\hbar^2}{2\pi\sqrt{M_1 M_2}} k'^2 \quad (10)$$

where k and k' represents the wave numbers of the electrically neutral mass mixtures in the collision direction. Inserting k , k' , ΔE and $\Delta E'$ from Eq. (11) into Eq. (10),

$$k = \left(\frac{2\pi}{2\Delta x}\right) = \frac{\pi}{\Delta x}, \quad k' = \frac{\pi}{\Delta x'}, \quad \Delta E = k_B T_c \quad \text{and} \quad \Delta E' = k_B T'_c \quad (11)$$

we get the following two formulas for transition temperatures:

$$T_c = \frac{\pi h^2}{4k_B} \frac{1}{\sqrt{M_1 M_2} \Delta x^2} \quad (12a)$$

$$T'_c = \frac{\pi h^2}{2k_B} \frac{1}{\sqrt{M_1 M_2} \Delta x'^2} \quad (12b)$$

where h and k_B represent the Planck constant, the Boltzmann constant, respectively. In the case of elastic atom-atom collisions Δx and $\Delta x'$ represent the length of the atomic mixture, that is $(a - (R_1 + R_2))$, where a is the distance between elastically colliding atoms or ions and R_1, R_2 are the corresponding radii. For elastic electron-atom collisions Δx and $\Delta x'$ represent the magnitudes $|\vec{R}|$ of direct lattice vectors. With the above **universal formulas** that differ from each other only by a factor of two, one can predict any critical temperature for any phase transition.

In this paper the transitions from normal conductivity to superconductivity are explained through the elastic atom-atom collisions. In some cases, superconductivity is caused by elastic collisions of n atoms or ions of the same element ($M_1 = M_2 = nM$) that move simultaneously and transmit their entire kinetic energy and momentum to the next group of n atoms. For calculating the superconducting transition temperatures I will utilise mainly the Eq. 12b, though in some cases I will apply both formulas. The ionic radii are the parameters that are used to fit the critical temperatures, but they are not allowed to excide the known experimental values. All other types of phase transitions are explained through elastic electron-atom collisions and transition temperatures are calculated by using the Eq. 12a.

3. Application of the T_C formulas

In the following sections, the transition temperatures for compounds that the author thinks are very interesting are calculated and compared with the experimental data.

3.1. Calculations of the superconducting transition temperatures by using the Eq. (12b)

In this paper, the transition temperatures for the multicomponent compounds of MgB_2 , $\text{La}_2\text{CuO}_{4+y}$, URu_2Si_2 and LaFePO will be calculated. Isotope effect, London's penetration lengths, critical magnetic fields and pressure effects will be treated in another paper. It is

important to point out that distances between the atoms of the same element during collisions do not vary continuously, but in general, they have the following three values: $2R$, R and $R/2$, where R is of the order of the empirical atomic radii (R_{Slater})⁸.

MgB₂ becomes superconducting at 39.4 K ^{9,10}; it adopts a hexagonal structure with space group $P6/mmm$ and lattice parameters of $a = 3.086\text{ \AA}$ and $c = 3.524\text{ \AA}$. In the following sections, all options of elastic atom-atom collisions that contribute to the onset of superconductivity are analyzed.

Boron chains: In all six *a*-directions, the vibration amplitudes in ...-B-B-B-... (see continuous black line in Fig. 2) chains is $\Delta x = (a - R_B/2)$, where R_B is the empirical atomic radius of boron. For these boron chains, we get 39.7 K for superconducting transition temperature.

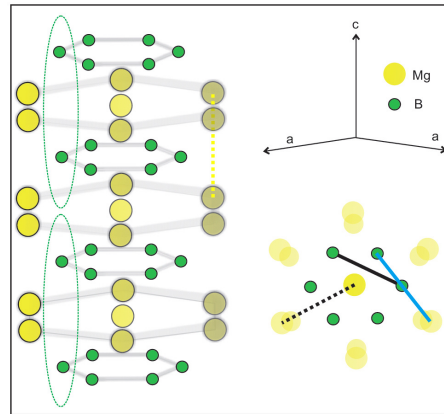


*Fig. 2: Crystal structure of MgB₂. Boron magnesium chains in *a*-directions and *c*-direction are labelled with the black continuous line, ellipses, dashed yellow and black lines respectively. The Mg-B-B chain is marked with the continuous blue line.*

It seems that in the *a*-directions, the elastic atom-atom collisions occur inside the molecular orbital, where boron behaves like a cation with atomic radius between 0.2 \AA and 0.25 \AA . This is in good agreement with the values of Pauling radius for B^{3+} and coordinate-type ion for B^{3+} . The T_c for $(a - R_{B(Slater)}/2)$, where $R_{B(Slater)} = 0.85\text{ \AA}$ becomes 39.1 K .

In *c*-direction, the vibrating “hard” boron ions have covalent radii $\langle R_B \rangle = (0.82\text{ \AA} + 0.84\text{ \AA})/2$, and $\Delta x = (c - 2\langle R_B \rangle)$. The vibrating B chains are ...-2B-2B-2B-... (see ellipses in Fig. 2) with masses $M_1 = M_2 = 2M_B$. After inserting M_1 , M_2 and Δx into the above universal formula 12b, we get 39.3 K as the superconducting transition temperature.

Mg chains: In all six *a*-directions, the vibrating Mg chains are ...-Mg²⁺- Mg²⁺- Mg²⁺- ... (see dashed line in Fig. 2). The radius of the “hard” Mg²⁺ ion is $0.66\text{ \AA} = R_{(Mg=Mg)}/2$, which is very

close to the Pauling radius of 0.65 \AA for Mg^{2+} . For $\Delta x = (a - 2R_{\text{Mg}^{2+}})$ and $M_1 = M_2 = Mg$, we get 39.4 K for T_c .

In c-direction, the “hard” Mg^{2+} radii are 0.881 \AA (this value is very close to the coordinate-type radii for Mg^{2+}), and $\Delta x = (c - 2R_{c-\text{Mg}^{2+}}) = c/2$; for these vibration amplitudes (see yellow dashed line in Fig. 2), we get a value of 39.5 K for superconducting T_c .

Mg-B-B chains in *a*-directions: In Fig. 2, these chains are labeled with blue line. There are two distances between the centers of atomic masses: the B-B distance $d_{B-B} = R_{B(\text{Slater})}/2$ and Mg-B $d_{\text{Mg-B}} = (R_{\text{Mg}(\text{Slater})}/2 + R_{B(\text{Slater})}/4)$. For $M_1 = M_B$, $M_2 = \sqrt{M_{\text{Mg}} M_B}$ and $\Delta x = [a - (d_{\text{Mg-B}} + d_{B-B})/2]$, we get a value of 39.4 K for critical temperature. As has been shown in an earlier work¹¹ with the ...-Mg-B-B-Mg-B-B-... chain, one can predict the isotope exponents for boron and magnesium.

La₂CuO_{4+y} is classified in the group of unconventional superconductors and has three transition temperatures^{12, 13}: $T_{c1} \approx 16 \text{ K}$, $32 \leq T_{c2} \leq 36 \text{ K}$, and $40 \leq T_{c3} \leq 45 \text{ K}$. The crystalline structure is orthorhombic with lattice parameters¹⁴ $a = 5.406 \text{ \AA}$, $b = 5.37 \text{ \AA}$, and $c = 13.15 \text{ \AA}$.

O chains: Along the $\langle 1, 1, 0 \rangle$ direction of real space, the shortest O-O distance is

$\sqrt{(a/2)^2 + (b/2)^2}$. For empirical covalent radius of $R_{\text{O}} = 0.73 \text{ \AA}$ ¹⁵, we imagine two types of O chains— the ...-O-O-O-... and the ...-2O-2O-2O-...— with masses $M_1 = M_2 = M_{\text{O}}$ and $M_1 = M_2 = 2M_{\text{O}}$ respectively. The maximal vibration amplitude for these vibrations is given as:

$\Delta x = (\sqrt{(a/2)^2 + (b/2)^2} - 2R_{\text{O}(a,b)})$. We get two T_c values that agree with the experimental results for T_{c1} , and T_{c2} : 16.8 K and 33.77 K for ...-2O-2O-2O-... and ...-O-O-O-... chains respectively.

Cu chains: The shortest Cu-Cu distance in $\langle 1, 1, 0 \rangle$ direction of real space is also equal to:

$\sqrt{(a/2)^2 + (b/2)^2}$. Similarly, for O chains, we imagine two types of copper “Newton cradles”: one ...-Cu-Cu-Cu-... and the other ...-2Cu-2Cu-2Cu-... with masses $M_1 = M_2 = M_{\text{Cu}}$ and $M_1 = M_2 = 2M_{\text{Cu}}$ respectively. The maximal vibration amplitude for copper vibrations is given as: $\Delta x = (\sqrt{(a/2)^2 + (b/2)^2} - 2R_{\text{Cu}(a,b)})$. The calculated T_c s for different types of Cu radii are listed in Table II.

TABLE II. Calculated transition temperatures for ...-Cu-Cu-Cu-... chain and different types of atomic radii. The atomic radii were obtained from Ref.¹⁵.

The type of Cu atomic radius	$R_{Cu} (\text{Å})$	$T_c^{calc} (K)$
van der Waals radius	1.4	46
Covalent radius (empirical)	1.38	42.6
Atomic radius (empirical)	1.35	38.1
Covalent radius (2008 values)	1.32	34.3

Vibrations of ...-2Cu-2Cu-2Cu-... chain give a T_c of 17 K that agrees with the experimental value of T_{c1} .

Cu-O chains: For vibrations in a - and b -directions, the ...-Cu-O-Cu-O-Cu-O-... chains may contribute to the onset of superconductivity. In a -direction, the Cu-O pairs vibrate with amplitudes of $\Delta x = [a - 2(R_{O^{2-}} + R_{Cu^{2+}})]$, and $M_1 = M_O$ and $M_2 = M_{Cu}$. For $R_{O^{2-}} = 1.24 \text{ Å}$ and $R_{Cu^{2+}} = 0.71 \text{ Å}$, we get a T_c of 41.3 K. In b -direction with $\Delta x = [b - 2(R_{O^{2-}} + R_{Cu^{2+}})]$, we get 43.3 K for T_c .

La-O chains: In $\langle 1,1,0 \rangle$ direction, the ...-La-O-La-O-La-O-... chains may contribute to the onset of superconductivity at 44 K for $M_1 = M_{La}$, $M_2 = M_O$, $R_{La} = 1.95 \text{ Å}$, $R_O = 0.66 \text{ Å}$ and $\Delta x = \left[\sqrt{(a/2)^2 + (b/2)^2} - (R_{La} + R_O) \right]$.

URu₂Si₂ becomes superconducting between 1.28 K and 1.4 K¹⁶. The lattice parameters for body-centered tetragonal URu₂Si₂ are: $a = b = 4.124 \text{ Å}$ and $c = 9.582 \text{ Å}$.

U chains: We get the best fit for transition temperature in U chains along $\langle 1,1,0 \rangle$ direction for $\Delta x = [\sqrt{2}a - 2R_U]$, with $R_U = 1.34 \text{ Å}$ (this is equal to the molecular double bond covalent radii) and $M_1 = M_2 = M_U$. The calculated T_c value for these elastic vibrations is 1.26 K.

In a -direction, the effective radii of the elastically vibrating U⁶⁺ cations are between 0.59 Å and 0.48 Å¹⁷. For $\Delta x = [a - 2R_{U^{6+}}]$, we get $T_c(0.59 \text{ Å}) = 1.44 \text{ K}$ and $T_c(0.48 \text{ Å}) = 1.25 \text{ K}$. This is expected since the most common oxidation number of uranium is +6¹⁵.

Ru chains: For maximal displacements along the $\langle 1,1,0 \rangle$ direction of real space

$\Delta x = [\sqrt{2}a - 2R_{Ru}]$, chain ...-2Ru-2Ru-2Ru-... and ruthenium radii of 1.25 Å, 1.26 Å, and 1.3 Å, we get $T_c(1.25 \text{ Å}) = 1.33 \text{ K}$, $T_c(1.26 \text{ Å}) = 1.34 \text{ K}$, and $T_c(1.30 \text{ Å}) = 1.41 \text{ K}$ respectively.

In a -direction, the vibrations of ruthenium cations are elastic.

Si chains: In c -direction, the elastic vibrations of Si⁴⁺ chains with ionic radii of 0.54 Å, 0.41 Å and 0.4 Å, and $\Delta x = [c - 2R_{Si^{4+}}]$, give T_c values of 1.377 K, 1.384 K and 1.47 K, respectively.

LaFePO is a superconductor with an onset transition temperature of 7.4 K¹⁸. The layered crystal structure of LaFePO is a tetragon of ZrCuSiAS type with lattice parameters

$a=3.9610(1) \text{ \AA}$ and $c=8.5158(2) \text{ \AA}$.

La chains: Along the $\langle 1,1,0 \rangle$ direction of real space, at the maximal vibration amplitude of $\Delta x = \left[\sqrt{2}a - 2R_{La} \right]$ with atomic radius $R_{La}=1.95 \text{ \AA}$, we calculate a T_c of 7.4 K.

Fe chains: Along the $\langle 1,1,0 \rangle$ direction of real space, at the maximal vibration amplitude of $\Delta x = \left[\sqrt{2}a - 2R_{Fe} \right]$ with atomic radius $R_{Fe}=1.4 \text{ \AA}$, we calculate a T_c of 6.8 K. In a -direction, for $R_{Fe^{3+}} = 0.63 \text{ \AA}$ and $\Delta x = \left[a - 2R_{Fe^{3+}} \right]$, we get a T_c of 7.3 K.

P chains: Along the $\langle 1,1,0 \rangle$ direction of real space, at the maximal vibration amplitude of $\Delta x = \left[\sqrt{2}a - 2R_p \right]$ with atomic radius $R_p=1.4 \text{ \AA}$, we calculate a T_c of 7.4 K.

O chains: Along the $\langle 1,1,0 \rangle$ direction, there are elastic intramolecular O-O collisions, where the minimal distance between oxygen mass centers is equal to the empirical atomic radius of oxygen that is 0.6 \AA . In this case, $\Delta x = \left[\sqrt{2}a - R_o \right]$, and we get a T_c of 7.4 K.

Other chains with different elements may also contribute to the collective quantum state of superconductivity in LaFePO.

3.2. Calculations of the superconducting transition temperatures by using the Eq. (12a)

Although the difference between formulas 12a and 12b is only one constant factor of two, they can give different information about the ionic or atomic radii and displacements. In the following I will calculate the transition temperatures for MgB_2 and La_2CuO_{4+y} , by using the formula 12a. As we will see below the formula 12a provide information about the oxidation states (oxidation number) of the ions.

Long time ago it was predicted that in **MgB₂** two B atoms accept two electrons from the Mg atoms so that a ionic compound of $Mg^{++}(B^-)_2$ result¹⁹. Therefore, in this compound we expect B ionic radii of the order of $r_{B^-} \geq r_{B^-Slater}$ and Mg ionic radii $r_{Mg^{++}} \leq r_{Mg^{++}Slater}$. In a -directions we get we get a T_c of 39.5 K, for $M_1=M_2=2M_B$ and $\Delta x = (a - 2R_B^a)$ with $R_B^a = 0.88 \text{ \AA} > R_B^{Slater}$. In c -direction we get a superconducting transition temperature of 39.6 K, for $M_1=M_2=2M_B$ and $\Delta x = (c - 2R_B^c)$ with $R_B^c = 0.825 \text{ \AA} \cong R_{emp.cov.rad.}$.

For Mg chains in a -directions we get a transition temperature of 39.4 K, for $M_1=M_2=M_{Mg}$ $\Delta x = (a - 2R_{Mg^{2+}}^a)$ where $R_{Mg^{2+}}^a = 0.917 \text{ \AA} < R_{Mg^{2+}}^{Slater}$. In c -direction we get a T_c of 39.35K

$M_1=M_2=M_{Mg}$ $\Delta x = (c - 2R_{Mg^{2+}}^c)$ where $R_{Mg^{2+}}^c = 1.135 \text{ \AA} < R_{Mg^{2+}}^{Slater}$.

As it was pointed out above there are three superconducting transition temperatures for **La₂CuO_{4+y}**, namely: $T_{c1} \approx 16 \text{ K}$, $32 \leq T_{c2} \leq 36 \text{ K}$, and $40 \leq T_{c3} \leq 45 \text{ K}$. Since in this compound

Cu atoms are positively charged and O atoms are negatively charged we expect

$$r_{O^{2-}} \geq r_{O-Slater} \text{ and } r_{Cu^{2+}} \leq r_{Cu-Slater}.$$

For elastic oxygen-oxygen collisions in a - and b -directions with: $M_1=M_2=M_O$,

$\Delta x = (a - 2R_O^a)$, $\Delta x = (b - 2R_O^b)$ and $R_O^a = R_O^b = R_{van-der-Waals} = 1.52 \text{ \AA}$ we get T_c -s of 16.7K and 17.3K, respectively.

Along $\langle 1,1,0 \rangle$ directions of real space the shortest O-O distance is

$$\sqrt{(a/2)^2 + (b/2)^2} = 3.8099 \text{ \AA}. \text{ For } M_1=M_2=M_O \Delta x = (\sqrt{(a/2)^2 + (b/2)^2} - 2R_{O^{2-}}^{\langle 1,1,0 \rangle}) \text{ we get}$$

transition temperatures as listed below.

TABLE III. Calculated T_c -s for ...-O²⁻- O²⁻-...chain along $\langle 1,1,0 \rangle$ directions.

$R_{O^{2-}}^{\langle 1,1,0 \rangle} (\text{ \AA})^{17}$	$T_c(\text{K})$
1.21	32
1.22	33
1.24	35
1.26	37
1.28	39.6

Along a - and b -directions the shortest Cu-Cu distances are $a/2$ and $b/2$. Elastic Cu-Cu collisions in a - and b -directions with: $M_1=M_2=M_{Cu}$, $\Delta x = (a/2 - 2R_{Cu^{2+}}^a)$,

$\Delta x = (b/2 - 2R_{Cu^{2+}}^b)$ and $R_{Cu^{2+}}^a = R_{Cu^{2+}}^b = 0.76 \text{ \AA}$ yield T_c -s of 16.7K and 17.4K, respectively.

Along $\langle 1,1,0 \rangle$ directions of real space the shortest Cu-Cu distances are

$$\sqrt{(a/2)^2 + (b/2)^2} = 3.8099 \text{ \AA}. \text{ For: } M_1=M_2=M_{Cu}, \Delta x = (\sqrt{(a/2)^2 + (b/2)^2} - 2R_{Cu}^{\langle 1,1,0 \rangle})$$

$R_{Cu}^{\langle 1,1,0 \rangle} = R_{Cu-covalent-radius(2008)} = 1.32 \text{ \AA}$ we calculate a T_c value of 17K.

3.3. Magnetism

In this section, we calculate the transition temperatures for these compounds: Fe, hexaboride CaB₆ and LaB₆, URu₂Si₂, UGe₂, UMn₂Al₂₀, Ni(C₂H₈N₂)₂NO₂(ClO₄), MgV₂O₄, CuCl₂

·2NC₅H₅, and Ba₃NbFe₃Si₂O₁₄. As mentioned above, the Δx s are the magnitudes of direct lattice vectors, which are equal to the distances within which the electron and atom masses are quasimixed.

Iron is the best-known ferromagnet with a Curie temperature of 1043 K. The crystal structure is body-centered cubic with a lattice constant of 2.866 \AA . For $\Delta x = 2.866 \text{ \AA}$, $M_I = M_{Fe}$ and m_e is equal to the free electron mass, we get a transition temperature of 1043 K.

Hexaboride compounds are very weak ferromagnets with small values of ordered magnetic moments and high Curie temperatures⁶. It was unexpected to find magnetic order in a material with no partially filled d - or f -orbitals. Later, it was found that there are iron impurities that are located on the crystalline surfaces and since the magnetic moments are confined within the sample surface, it was supposed that the magnetic order is not intrinsic^{4,20}. On the other

hand, the NMR experiments²¹ and the lack of dependency of measured ordered moment on the iron concentration in the flux⁵ suggest that ferromagnetism in hexaboride is not only on the surface, but is also a bulk property. In the following, it is proved that both these opinions are valid, i.e., iron impurities on the surface are magnetically ordered, but the magnetic order is itinerant.

In Fig. 3, it is shown how FeB and Fe₂B molecules on sample surface are connected with each other through elastic boron-electron collisions within the hexaboride crystal.

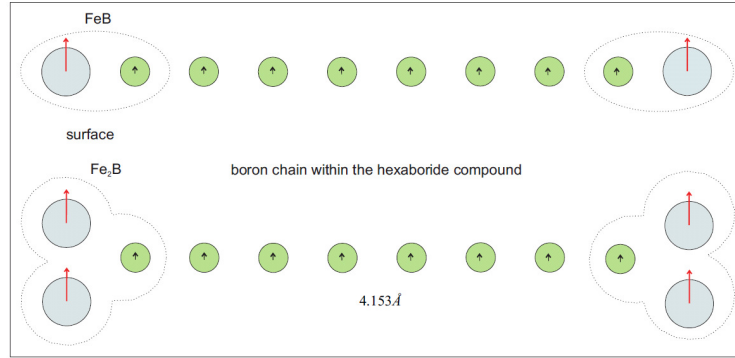


Fig. 3: Hyperexchange interconnection between magnetic moments in FeB and Fe₂B molecules are caused through the elastic boron-electron collisions within the 1D boron chains. The Curie temperatures for FeB and Fe₂B compounds are ~598 K and ~1015 K respectively⁴.

CaB₆ and LaB₆ are ferromagnetic and each compound shows two ferromagnetic phase transitions with Curie temperatures⁴: $T_{c1}(\text{CaB}_6) \approx 600$ K, $T_{c2}(\text{CaB}_6) \approx 1100$ K, $T_{c1}(\text{LaB}_6) \approx 600$ K and $T_{c2}(\text{LaB}_6) \approx 1100$ K. Both compounds have cubic structures with lattice constants of $a_{\text{CaB}_6} \approx 4.153$ Å and $a_{\text{LaB}_6} \approx 4.156$ Å. First, let us calculate the transition temperatures for elastic boron-electron collisions. For $\Delta x_{\text{CaB}_6} = 4.153$ Å, $\Delta x_{\text{LaB}_6} = 4.156$ Å, $M_1 = M_B$ and $M_2 = m_e$, we get a T_c s of 1128 K and 1126 K for CaB₆ and LaB₆ respectively. These values agree with the experimental values for T_{c2} .

Along the $\langle 1,1,0 \rangle$ direction of real space, we get $T_{c1}(\text{CaB}_6) = 564$ K and $T_{c1}(\text{LaB}_6) = 563$ K for boron chains. In CaB₆, the elastic Ca-electron collisions in Ca chains in a -direction ($\Delta x_{\text{CaB}_6} = 4.153$ Å) yield a value of 586 K, which agree with the experimental value of $T_{c1}(\text{CaB}_6)$.

In LaB₆, the elastic (LaB)-electron collisions in LaB chains in a -direction ($\Delta x_{\text{LaB}_6} = 4.156$ Å) with $M_1 = \sqrt{M_{\text{La}} M_B}$ and $M_2 = m_e$ yield a value of 595 K, which agrees with the experimental value of $T_{c1}(\text{LaB}_6)$. Based on this scenario, both opinions, namely, the itinerant and surface origin of magnetic order in hexaboride compounds, are plausible. Since boron, calcium and

lanthanum atoms do not possess electric magnetic moments, the ferromagnetic order of nuclear magnetic moments along the 1D atom chains might be a possible scenario for these materials.

URu₂Si₂ exhibits an enigmatic phase transition at 17.5 K to a “hidden-order” state for which the order parameter remains unknown even after 25 years of intense research. It is interesting that although a lot of experimental investigations had been carried out with different techniques to understand the phase transition at 17.5 K, it remained mysterious till now. In the present case, we claim that if we do not have the right theoretical tools, the experiments alone can not help us to understand the physical phenomena. Hence, we apply the universal formula 12a for phase transitions and find out which elastic electron-atom collisions cause a transition at 17.5 K.

In Table III, all elastic electron-atom collisions in different directions are listed. The electron mass m_e is taken to be equal to the mass of free electron and $\Delta x = |\vec{R}|$.

TABLE IV. Calculated transition temperatures for all possible elastic collisions of electrons with Ru, Si and RuSi atoms in different crystalline directions.

M_I	\vec{R}	$T_c^{calc} (K)$
M_{Ru}	$2\vec{c}$	17.5
M_{Ru}	$4\vec{a} + \vec{c}$	17.5
M_{Si}	$3\vec{a} + 3\vec{b} + 2\vec{c}$	17.9
$\sqrt{M_{Ru}M_{Si}}$	$2\vec{a} + 2\vec{b} + 2\vec{c}$	17.5

For direct lattice vectors $\vec{R}_i = 2\vec{a} + 2\vec{b} + \vec{c}$, $\vec{R}_j = 3\vec{a} + \vec{c}$ and $\vec{R}_k = 3\vec{b} + \vec{c}$, the elastic electron-uranium collisions yield two values for transition temperatures, namely 18.2 K and 16.9 K. Since every uranium atom is connected with 16 other U atoms (see Fig. 4)– eight times by direct lattice vectors of lengths $|\vec{R}_i|$ and eight times by direct lattice vectors of lengths $|\vec{R}_j|$ and $|\vec{R}_k|$ – for these two lengths, we get a mean value of $\langle T_c(U) \rangle = (8 \cdot 18.2 \text{ K} + 8 \cdot 16.9 \text{ K}) / 16 = 17.5 \text{ K}$.

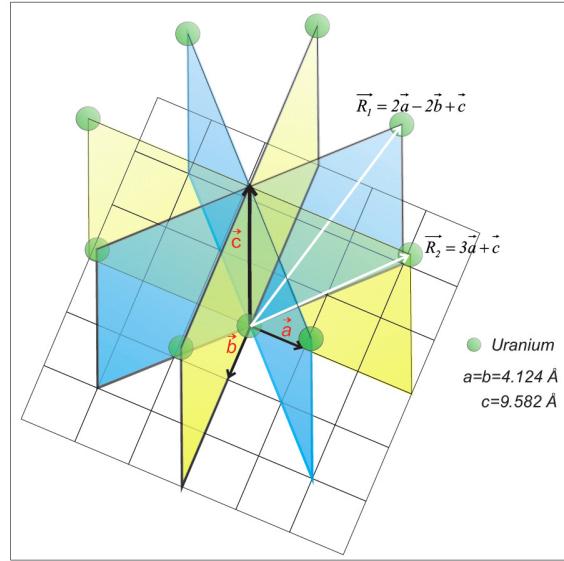


Fig. 4: Parallel to the diagonals of the blue and yellow areas, the elastic electron-uranium collisions contribute to the “most enigmatic” phase transition at 17.5 K.

In $\langle 1,1,0 \rangle$ direction with $\vec{R} = \vec{a} + \vec{b}$, the phase transition at 17.5 K may also be induced by elastic “heavy electron”-uranium collisions. Experimentally, it was found that at low temperatures, the effective mass of heavy electrons is $m_e \approx 50m_0$ ²² where m_0 is the free electron mass. After inserting $\Delta x = |\vec{a} + \vec{b}|$, $M_1 = M_U$, and $m_e \approx 50m_0$ into the universal formula 12a, we get a T_c of 17.25 K.

UGe₂: become ferromagnetic below Curie temperature of 52K²³. The lattice parameters for orthorhombic UGe₂ are: $a = 4.11 \text{ \AA}$, $b = 15.10 \text{ \AA}$ and $c = 3.97 \text{ \AA}$ ²³. For: $\Delta x_U = |\vec{a} + 2\vec{c}|$,

$\Delta x_{Ge} = |3\vec{c}|$, $M_1 = M_U$, $M_1 = M_{Ge}$ and $M_2 = 1m_0$ we get transition temperatures of 52K and 52.9K, respectively. In c-direction the magnetic order is induced by elastic “heavy electron”-uranium collisions. After inserting $\Delta x = |\vec{c}|$, $M_1 = M_U$, and $M_2 = m_e \approx 25m_0$ ²³ into the universal formula 12a, we get a T_c of 52.6K.

UMn₂Al₂₀: is a ferromagnet with Curie temperature of 20K²⁴. The lattice constant of this cubic compound is 14.319 \AA ²⁴. For: $M_2 = m_e$, $\Delta x_U = |\vec{a}|$, $\Delta x_{Mn} = |\vec{a} + \vec{a}|$, $\Delta x_{Al} = |\vec{a} + \vec{a} + \vec{a}|$ and $M_1 = M_U$, $M_1 = M_{Mn}$, $M_1 = M_{Al}$ we get transition temperatures of 20.2K, 20.9K and 20K, respectively.

Ni(C₂H₈N₂)₂NO₂(ClO₄) has an orthorhombic crystalline structure with the lattice parameters $a = 15.223 \text{ \AA}$, $b = 10.300 \text{ \AA}$, and $c = 8.295 \text{ \AA}$ ²⁵. The experimental values for exchange

interactions are between ~ 48 K and ~ 43 K^{25,26}. In Table IV, the contributions for each element are listed. It is interesting that for each element, it is easy to find the right direct lattice vector that exactly fits the experimental values for T_c s.

TABLE V. Calculated transition temperatures for all possible elastic collisions of electrons with Ni, O, H, Cl, C and N chains in different crystalline directions.

M_I	\vec{R}	T_c^{calc} (K)
M_{Ni}	$\vec{b} + \vec{c}$	47.6
M_O	$\vec{a} + \vec{b}$	47.4
M_H	$2\vec{a} + 2\vec{c}$	47.4
M_{Cl}	\vec{a}	46.4
M_C	$2\vec{b}$	43.5
M_N	$\vec{a} + \vec{b} + \vec{c}$	42
M_N	$\vec{b} + 2\vec{c}$	45

There might be other possible direct lattice vectors and atom-atom mass mixing that can exactly fit the experimental values for critical temperatures.

MgV₂O₄: At approximately ~ 65 K²⁷, this compound undergoes a structural phase transition from cubic to tetragonal shape. Below ~ 42 K²⁷, a long-range antiferromagnetic order of magnetic moments occurs. The lattice parameters of tetragonal phase are $a=b \approx 5.96047$ Å, $c \approx 8.37927$ Å²⁷. In Table V, the calculated T_c values are listed for elastic electron-vanadium, electron-oxygen and electron-magnesium collisions in different orientations.

TABLE VI. Calculated T_c s for all possible elastic collisions of electrons with V, O and Mg atoms in different crystalline directions.

M_I	\vec{R}	T_c^{calc} (K)
M_V	$2\vec{a}$	63
M_V	$2\vec{a} + \vec{c}$	42.2
M_O	$2\vec{a} + \vec{b} + \vec{c}$	64.5
M_O	$2\vec{a} + 2\vec{b} + \vec{c}$	45
M_O	$\vec{a} + \vec{b} + 2\vec{c}$	45

$\sqrt{M_V M_O}$	$2\vec{c}$	42.6
M_{Mg}	$2\vec{a} + \vec{c}$	61.2
M_{Mg}	$\vec{a} + 2\vec{c}$	41

CuCl₂·2NC₅H₅: The best fit of magnetic susceptibility versus temperature yield a value of the intrachain Heisenberg coupling of 27.3 K²⁸. The lattice parameters of monoclinic dichlorobis (pyridine) copper (II) are: $a = 17.00 \text{ \AA}$, $b = 8.59 \text{ \AA}$, and $c = 3.87 \text{ \AA}$ ²⁹. Calculated T_c s for all elements in different crystalline orientations are given in Table VI.

TABLE VII. Calculated T_c s for all possible elastic collisions of electrons with Cu, Cl, N, C, and H atoms in different crystalline directions.

M_I	\vec{R}	$T_c^{calc} (K)$
M_{Cu}	\vec{a}	27.7
M_{Cu}	$2\vec{b}$	27.2
M_{Cl}	$\vec{a} + \vec{b} + \vec{c}$	28.4
M_N	$\vec{a} + 2\vec{b}$	29.2
M_C	$3\vec{b}$	27.8
M_H	$2\vec{a} + 4\vec{b}$	27.4

Ba₃NbFe₃Si₂O₁₄ is a multiferroic with experimental transition temperature between 26 K³⁰ and 27 K³¹. This compound crystallizes in a hexagonal noncentrosymmetric P321 structure. The experimental results reveal two slightly different phases with two groups of lattice parameters, namely, $a=b \approx 8.6049 \text{ \AA}$ and $c \approx 5.2523 \text{ \AA}$ ³⁰, and $a'=b' \approx 8.6049 \text{ \AA}$ and $c' \approx 5.2523 \text{ \AA}$ ³¹. Contributions of each element to the onset of phase transition are listed in Table VII.

TABLE VIII. Calculated T_c s for elastic collisions of electrons with Ba, Nb, Fe, Si, and O atoms in different crystalline directions.

M_I	\vec{R}	$T_c^{calc} (K)$
M_{Ba}	$\vec{a}' + \vec{b}'$	26.07
M_{Nb}	$3\vec{c}$	27.7
M_{Fe}	$\vec{a} + \vec{b} + 2\vec{c}$	26
M_{Si}	$4\vec{c}$	27
M_O	$3\vec{a}'$	25.5

One can also fit the transition temperature by mixing the atomic masses of different elements.

3.4. Spontaneous electric polarization

In this section, the transition temperatures will be calculated for the following compounds: $\text{Bi}_4\text{Ti}_3\text{O}_{12}$, $\text{K}_3\text{WO}_3\text{F}_3$ and $\text{Ba}_2\text{Bi}_4\text{Ti}_5\text{O}_{18}$.

$\text{Bi}_4\text{Ti}_3\text{O}_{12}$ is a ferroelectric with a Curie temperature of 948 K³². The lattice parameters of orthorhombic crystalline structure are: $a \approx 5.448 \text{ \AA}$, $b \approx 4.110 \text{ \AA}$ and $c \approx 32.830 \text{ \AA}$ ³³. Along b -direction with $\Delta x = 4.11 \text{ \AA}$ and $M_I = M_O$, the elastic electron-oxygen collisions yield a T_c of 947.4 K.

We get exactly the same value of 947.4 K for monoclinic layer-perovskite structure with lattice parameters of $a' \approx 5.450 \text{ \AA}$, $b' \approx 5.4059 \text{ \AA}$ and $c' \approx 32.832 \text{ \AA}$ ³⁴ along the $\langle 1, 1, 0 \rangle$ direction of real space for ...-(OTi-O)-(OTi-O)-(OTi-O)-... chain. In this chain, titanium atoms are closer to one oxygen atom than to the other. The mixed atomic mass for OTi-O triad is given as $M_I = \sqrt{\sqrt{M_O M_{Ti}} M_O}$ and the Δx for elastic electron-(OTi-O) collisions is $(\sqrt{a'^2 + b'^2} / 2)$.

$\text{K}_3\text{WO}_3\text{F}_3$ becomes ferroelectric at $T_{c1} = 414 \text{ K}$ and $T_{c2} = 455 \text{ K}$ ³⁵. The crystalline structure is monoclinic with lattice parameters given as: $a \approx 8.7350 \text{ \AA}$, $b \approx 8.6808 \text{ \AA}$, and $c \approx 6.1581 \text{ \AA}$ and angle of $\beta = 135.124^\circ$. Along c -direction with $\Delta x = 6.1581 \text{ \AA}$ and $M_I = M_O$, the elastic electron-oxygen collisions yield a T_c of 422 K, which lies between two experimental values. We calculate a transition temperature of 416 K along the $\langle 1, 1, 0 \rangle$ direction of real space for ...-(OW-O)-(OW-O)-(OW-O)-... chain. In this chain, tungsten atoms are closer to one oxygen atom than the other. The mixed atomic mass for OW-O triad is given as

$M_I = \sqrt{\sqrt{M_O M_W} M_O}$ and the Δx for elastic electron-(OW-O) collisions is $(\sqrt{a^2 + b^2} / 2)$.

There are other options too that fit the experimental Curie temperatures. For example, for

$\Delta x = a/2$ and $M_I = \sqrt{M_O M_W}$, we get a value of 455 K. For $\Delta x = (\sqrt{a^2 + b^2} / 2)$ and

$M_I = \sqrt{M_K M_F}$, we get 433 K as the transition temperature.

$\text{Ba}_2\text{Bi}_4\text{Ti}_5\text{O}_{18}$ is tetragonal with lattice parameters $a = b \approx 3.88 \text{ \AA}$ and $c \approx 50.3 \text{ \AA}$ ³⁶. The experimental values for transition temperature are between 597 K and 602 K³⁶. The most recent experimental results, however, reveal a T_c of 633 K³⁷. Along a - and b -directions ($\Delta x = a$ and $\Delta x = b$), the 1D titanium chains yield a value of 614 K. For BaO chain with

$M_I = \sqrt{M_O M_{Ba}}$ along a - and b -directions, we get a value of 625 K, which is in agreement

with recent experimental results. It is impossible to fit the Curie temperature from the crystalline structure for the OBi-O chains. Therefore, for this atomic triad with mixed mass of

$M_I = \sqrt{\sqrt{M_O M_{Bi}} M_O}$, we take, for Δx , the sum of BiBi and OO bond lengths, which is equal to 4.29 Å. After inserting these values into the universal formula 12a, we get a T_c of 629 K, which is in excellent agreement with the recent experimental results. More calculations on phase transitions between ordered and disordered states of electric dipoles can be found in my unpublished work³⁸.

3.5. Crystallization (melting)

First, two transition temperatures of extremely different energy scales, namely, the melting point of ⁸⁷Rb optical lattice and the melting point of diamond are calculated.

⁸⁷Rb optical lattice: At very low temperatures through Bose-Einstein condensation (BEC), two rubidium atoms at each lattice site are confined to a 3D optical lattice with a wavelength (lattice constant) of 830.44 nm³⁹. This wavelength is equal to the separation distance (Δx) between two neighboring rubidium pairs. At temperatures below $T_c \approx 240$ nK⁴⁰, the phase transition to an ordered optical lattice (BEC) occurs. For $M_I = 2M_{Rb}$, $M_2 = 2M_{Rb}$ and $\Delta x = 830.44$ nm, we calculate a transition temperature of 250 nK that is in excellent agreement with the experimental value of 240 nK.

Diamond: The lattice of diamond consists of two interpenetrating face-centered cubic lattices; the lattice constant is $a = 3.566$ Å. Until now, we have generally spoken about the elastic electron-atom collisions; however, in p-type semiconductors, we have elastic hole-atom collisions. The average effective mass of heavy holes in diamond is $0.574m_0$ ⁴¹ (m_0 is the mass of free electron). The experimental value for solid-liquid transition temperature of diamond is ~ 3823 K. For $M_I = M_C$, $M_2 = 0.574m_0$ and $\Delta x = (\sqrt{2}/2)a$, the universal formula 12a yields a value of 3836 K.

In Table VIII, the calculated values for solid-liquid transition temperatures for different semiconductors are given.

TABLE IX. Calculated solid-liquid temperatures for semiconducting materials with effective mass smaller than the free electron mass.

	M_I	M_2	Δx	T_c^{calc} (K)	T_c^{exp} (K)
HgSe	M_{Se}	$\sim 0.035m_0$	$a = 6.0853$ Å	1039	1063
AlAs	M_{Al}	$\sim 0.150m_0$	$(\sqrt{2}/2)a$; $a = 5.66$ Å	1987	1993
BP	$\sqrt{M_B M_P}$	$\sim 0.200m_0$	$(\sqrt{2}/2)a$; $a = 4.538$ Å	3244	3300

3C-SiC	M_{Si}	$\sim 0.156m_0$	$(\sqrt{2}/2)a$; $a=4.359\text{\AA}$	3200	3103
Ge	M_{Ge}	$\langle 1,1,0 \rangle$ direction $\sim 0.153m_0$	$(\sqrt{2}/2)a$; $a=5.657\text{\AA}$	1200	1211
Si	M_{Si}	$\langle 1,1,0 \rangle$ direction $\sim 0.25m_0$	$(\sqrt{2}/2)a$; $a=5.657\text{\AA}$	1638	1687
SiO ₂	$\sqrt{M_{Si}M_o}$	$\sim 0.500m_0$	$d_{Si-o-Si}=3.13\text{\AA}$	1932	1983
ZnO	$\sqrt{M_{Zn}M_o}$	$\sim 0.190m_0$	$a=3.25\text{\AA}$	2444	2521; 2248

A detailed analysis of solid-liquid and liquid-gas phase transitions requires extensive work that is out of the scope of this paper.

4. Discussion and Conclusion

In this paper, a new simple and universal theoretical model that is able to predict the critical temperatures for any phase transition is presented. With this new model, the analogy between conventional and unconventional superconductivity is proven. The origin of weak ferromagnetism with high Curie temperatures in CaB₆ and LaB₆ as well as the origin of phase transition at 17.5 K in URu₂Si₂ are explained. It has been shown that magnetic order may also be induced from elastic collisions between electrons and atoms that do not possess local magnetic moments, i.e. with no partially filled *d*- or *f*-orbitals, such as CaB₆ and LaB₆.

Why is the model of elastic electron-atom and atom-atom collisions universal and why is it able to predict any phase transition? There are probably three main reasons. The first one is that this model is based directly on the fundamental conservation laws of energy and momentum, and since any phase transition is of quantum mechanical origin, the application of Schrödinger equation and Heisenberg's uncertainty principle are the right tools to crack the "secret code" of any phase transition. The second reason could be that the model is based on the universal electrical neutrality, which is a simple fact that we know from our everyday life. The third reason could follow from the fact that we have two fundamental constants, namely, the Planck constant *h* and the Boltzmann constant *k_B* that connect the crystalline structure with kinetic energy and kinetic energy with temperature, respectively.

In this paper, I have shown that to understand unconventional superconductivity and any other phase transition, we do not need a new revolution; all we need is one logical combination of the simple facts that we know from our basic physical knowledge.

I end this paper with a question that can be answered only experimentally:

Do the electrically neutral particles with masses $\sqrt{m_e M}$ (for instance $M=M_{Fe}$ and $m_e=m_0$
 $\sqrt{m_e M} = 320m_0$) exist independently, or are they just confined inside the many particle
systems?

Acknowledgment

I would like to thank Prof. Pekka Pyykkö for enlightening discussions on atomic radii.

References:

- 1 J. Zaanen, S. Chakravarty, T. Senthil, et al., *Nature Physics* **2**, 138 (2006).
- 2 S. Chakravarty, *Science* **266**, 386 (1994).
- 3 S. Q. Wang, W. E. Evenson, and J. R. Schrieffer, *Phys. Rev. Lett.* **23**, 92 (1969).
- 4 K. Matsubayashi, M. Maki, T. Tsuzuki, et al., *Nature* **420**, 143 (2002).
- 5 D. P. Young, Z. Fisk, J. D. Thompson, et al., *Nature* **420** (2002).
- 6 D. P. Young, D. Hall, M. E. Torelli, et al., *Nature* **397**, 412 (1999).
- 7 B. A. Strukov and A. P. Levanyuk, *Ferroelectric Phenomena in Crystals* (Springer, Madrid, Moscow, 1997).
- 8 J. C. Slater, *J. Chem. Phys.* **41**, 3199 (1964).
- 9 J. Nagamatsu, N. Nakagawa, T. Muranaka, et al., *Nature* **410**, 63 (2001).
- 10 J.-C. Zheng and Y. Zhu, *Phys. Rev. B* **73**, 024509 (2006).
- 11 S. Mushkolaj, arXiv:0810.4265v1 (2008).
- 12 M. Fratini, N. Poccia, A. Ricci, et al., *Nature* **466**, 841 (2010).
- 13 Q. Y. Tu, X. L. Chen, B. K. Ma, et al., *Physica C* **370**, 94 (2002).
- 14 V. B. Grande, H. Müller-Buschbaum, and M. Schweizer, *Z. Anorg. Allg. Chem.* **428**, 120 (1977).
- 15 www.webelements.com.
- 16 F. Bourdarot, E. Hassinger, S. Raymond, et al., *J. Phys. Soc. Jpn.* **79**, 094706 (2010).
- 17 R. D. Shannon and C. T. Prewitt, *Acta Cryst.* **B25**, 925 (1969).
- 18 M. Yamashita, N. Nakata, Y. Senshu, et al., *Phys. Rev. B* **80**, 220509 (2009).
- 19 W. N. Lipscomb and D. Britton, *J. Chem. Phys.* **33**, 275 (1960).
- 20 K. Taniguchi, T. Katsufuji, F. Sakai, et al., *Phys. Rev. B* **66**, 064407 (2002).
- 21 S. Mushkolaj, Diss. ETHNo. 15936 (2005).
- 22 W. Schlabit, J. Baumann, B. Pollit, et al., *Z. Phys. B-Condensed Matter* **62**, 171 (1986).
- 23 K. K. Satoh, S. W. S.W. Yun, I. I. Ukon, et al., *J. Magn. Magn. Mater.* **104-107**, 39 (1992).
- 24 C. H. Wang, J. M. Lawrence, E. D. Bauer, et al., *Phys. Rev. B* **82**, 094406 (2010).
- 25 A. V. Sologubenko, T. Lorenz, J. A. Mydosh, et al., *Phys. Rev. Lett.* **100**, 137202 (2008).
- 26 H. Huang and I. Affleck, *Phys. Rev. B* **69**, 184414 (2004).
- 27 E. M. Wheeler, B. Lake, A. T. M. N. Islam, et al., *Phys. Rev. B* **82**, 140406(R) (2010).
- 28 J. A. Chakhalian, R. F. Kiefl, R. Miller, et al., *Phys. Rev. Lett.* **91**, 027202 (2003).
- 29 W. Duffy Jr., J. E. Venneman, D. L. Strandburg, et al., *Phys. Rev. B* **9**, 2220 (1974).
- 30 H. D. Zhou, L. L. Lumata, P. L. Kuhns, et al., *Chem. Mater.* **21**, 156 (2009).
- 31 K. Marty, V. Simonet, E. Ressouche, et al., *Phys. Rev. Lett.* **101**, 247201 (2008).
- 32 T. Hirata and T. Yokokawa, *Solid State Communications* **104**, 673 (1997).

- 33 B. D. Stojanovic, C. O. Paiva-Santos, M. Cilense, et al., *Materials Research Bulletin* **43**, 1743 (2008).
- 34 X. Q. Pan, J. C. Jiang, C. D. Theis, et al., *App. Phys. Lett.* **83**, 2315 (2003).
- 35 V. V. Atuchin, T. A. Gavrilova, V. G. Kesler, et al., *Chem. Phys. Lett.* **493**, 83 (2010).
- 36 B. Aurivillius and P. H. Fang, *Phys. Rev.* **126**, 893 (1962).
- 37 H. Irie, M. Miyayama, and T. Kudo, *J. Am. Ceram. Soc.* **83**, 2699 (2000).
- 38 S. Mushkolaj, arXiv:0810.4088v1 (2008).
- 39 N. Syassen, D. M. Bauer, M. Lettner, et al., *Science* **320**, 1329 (2008).
- 40 S. Burger, F. S. Cataliotti, C. Fort, et al., *Europhys. Lett.* **57**, 1 (2002).
- 41 R. Sauer, N. Teofilov, and K. Thonke, *Diamond and Related Materials* **13**, 691 (2004).